The Journal of the Oceanological Society of Korea
Vol. 27, No. 3, pp. 189-196, September 1992

A Simple Model for Separation of East Korean Warm Current and Formation of North Korean Cold Current

YOUNG HO SEUNG
Dept. of Oceanography, Inha Univ., Inchon 402-751, Korea

동한난류의 이안 및 북한한류의 형성에 관한 단순모델

승 영 호
인하대학교 해양학과

A simple quasi-geostrophic model is considered to explain the separation of the East Korean Warm Current(EKWC) and formation of the North Korean Cold Current(NKCC). In this model, the circulation is driven by inflow-outflow condition and modified by local forcing. The solution is decomposed into inflow-outflow and local modes which describe only the effects of inflow-outflow condition and local forcing, respectively. Results of analyses show that both the surface cooling and positive wind stress curl are favorable for the separation of EKWC and formation of NKCC. This fact is compatible with the present knowledge about heat flux and wind stress field over the Sea of Japan.

동한난류의 이안 및 북한한류의 생성을 규명하기 위하여 간단한 역학모델을 수립하였다. 본 모델에서는 해류가 유입-유출 조건에 의하여 형성되고 국지적인 힘에 의해 변형된다. 기본방정식의 해로서 유입-유출에 의해서만 형성되는 유입-유출 모드와 국지적인 힘에 의해서만 형성되는 국지 모드를 얻었다. 분석결과, 표면냉각과 양의 부호를 갖는 바람응력와도가 동한난류이안 및 북한한류형성을 일으킴이 밝혀졌다. 이 사실은 동해에서의 열교환 및 바람응력장에 대하여 현재까지 알려진 바와 부합된다.

INTRODUCTION

The major feature of the circulation of the Sea of Japan is the inflow of warm water through the Korea Strait and outflow through the Tsugaru and Soya Straits(Fig. 1). Though some parts of it flow along the Japanese coast due to the topographic control, much of it flows northward along the Korean coast forming the East Korean Warm Current (briefly, EKWC). A prominent feature of the East Sea circulation is that the EKWC separates from the shore near 38°N then flows nearly in zonal direction until it finally drains out through the outlets. North of the warm current region, a cold current called the North Korean Cold Current(briefly, NKCC) or Liman Current flows southward along the western boundary and separates from the shore where it meets with the EKWC. It seems that the point of separation is largely determined by the condition of surface heat flux. This fact is partly supported by observations (Hong et al.,1984; Kim and Legeckis,1986) where an abnormal cold water moved far to the south, with corresponding strong thermal front, in Spring-Summer,1981 following the severe Winter.The NKCC, after separation, seems to form a recirculating cyclonic gyre in the north of the warm current region(Uda, 1934; U.S.Navy, 1977; Hydrographic office of Korea, 1982). Geostrophic computations made by Lim and An (1985) also indicate the presence of recirculation in the north. These facts are schematized in Fig. 1.

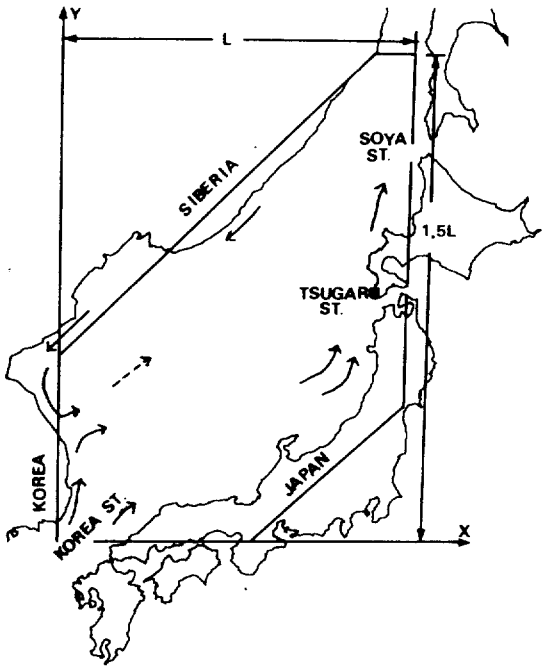

Fig. 1. Idealization of the East (Japan) Sea with horizontal coordinate system. Arrows are schematic presentation of the current path.

Numerical studies by Yoon(1982a and b) do not succeed in showing the formation of the NKCC and the separation of EKWC. Sekine(1986) also considers the wind stress curl in his model but the results seem to be insufficient to explain the separation of EKWC and formation of NKCC. Seung and Kim(1989) emphasized the role of buoyancy flux in formation of the NKCC and the separation of EKWC. In Seung and Kim(briefly, SK), the effect of buoyancy flux is parameterized by using the concept of "basic buoyancy structure" of the East Sea which would be induced by adjustment of the basin to local thermal forcing in the absence of circulation.

Present study aims at clarifying the dynamics of separation of EKWC and formation of NKCC in continuation of SK's study. For this purpose, the circulation is decomposed into the inflow-outflow driven mode(briefly, IM) and locally driven mode(briefly, LM). This approach allows one to understand, and measure the importance of the relative role of local forcing in the circulation of the East Sea. The local forcing here includes both the surface heat(buoyancy) flux and the wind stress curl.

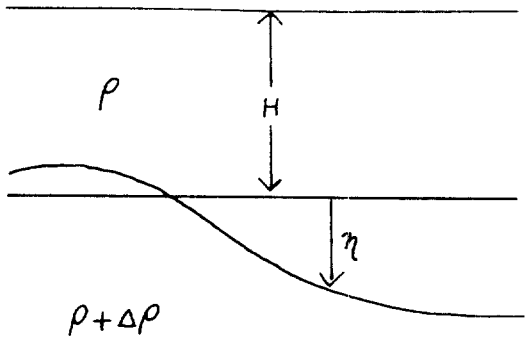

Fig. 2. Definition sketch of the two-layer ocean.

FORMULATION

The problem considered here is almost the same as SK(1989)and detailed explanation is not given here. Take a two-layer ocean with motionless deep lower layer(Fig. 2). The surface is assumed to be rigid-lid and motions are induced by small perturbation. The coordinate system is such that x orients eastward; y, northward; and z, upward (Fig. 1). On the beta-plane, the governing equation of motion is

$$\frac{D\vec{u}}{Dt} = -f\vec{n}\times\vec{v} - g'\nabla\eta - K\vec{u} + \frac{\vec{\tau}}{\rho H} \qquad (1)$$

where $\frac{D}{Dt}$ is the total derivative; $\vec{u}$, horizontal velocity vector in the upper layer; $\vec{n}$, upward unit vector; $g'=g\nabla\rho/\rho$, the reduced gravity; g, the gravity constant; ρ, upper layer density ; $\Delta\rho$, vertical density difference; η, interface depression; K, linear friction coefficient; $\vec{\tau}$, wind stress vector; and H, upper layer thickness. In quasi-geostrophic assumption, the first order balance in Eq.(1) is between the first two terms on the right hand side. All other terms have the second order of magnitude. The equation describing the lowest order vorticity balance is obtained from Eq.(1) as follows.

$$\frac{\partial\zeta_g}{\partial t} + f_o\nabla\cdot\vec{u}_a + \vec{u}_g\cdot\nabla\zeta_g + v_g\beta = -K\zeta_g + \frac{\vec{n}\cdot curl\vec{\tau}}{\rho H} \qquad (2)$$

where ζ_g is the geostrophic vorticity; f_o, the Coriolis' parameter at y=0; $\vec{u}_a$, ageostrophic component of velocity which is an order smaller than the geostrophic component $\vec{u}_g$; v_g, the y-component of geostrophic current; and β, the northward gradient of the Coriolis' parameter.

The continuity equation is the balance among the second order terms, i.e., time variation of interface elevation, divergence induced by ageostrophic component of current and the effect of buoyancy (heat) flux. The effect of buoyancy flux is parameterized here by conversion of water, i.e., from upper to lower layer waters if cooling is envolved and vice versa. This parameterization seems to be more realistic than that in SK. The continuity equation then becomes

$$\frac{\partial \eta}{\partial t} + H\nabla \cdot \vec{u}_a = -Wc \tag{3}$$

where Wc is the conversion rate from upper to lower waters due to surface cooling. The negative value means surface heating. Steady state form of Eq.(3) shows that the surface cooling(heating) has the same effect as the horizontal convergence(divergence), thus resulting in vortex stretching. Eq.(3) and Eq.(2), with the use of geostrophic stream function defined by

$$\vec{u}_g = \vec{n} \times \nabla \psi = \vec{n} \times \nabla \left[\frac{g' \eta}{f_o} \right] \tag{4}$$

leads to the vorticity equation as follows:

$$\frac{\partial}{\partial t}\left[\nabla^2 - \frac{1}{R^2}\right]\psi + J(\psi, \nabla^2\psi) = \frac{f_o}{H} Wc - \beta \frac{\partial \psi}{\partial x} - K\nabla^2\psi + \vec{n} \cdot \mathrm{curl}\vec{\tau}/\rho H \tag{5}$$

where $R = \sqrt{g'H}\,/fo$ is the Rossby radius and J represents the Jacobian operator. For linear and steady state circulation, the first two terms in the left hand side can be ignored. For convenience, nondimensionalization is made with respect to the length scale L(east-west dimension of the basin) and the interior velocity scale U so that distance variables and stream function are normalized by L and UL, respectively. The result is

$$\frac{\partial \psi}{\partial x} + C\nabla^2\psi = F \tag{6}$$

$$F = f_o(Wc + We)/H\beta U$$

where $C = K/\beta L$, and $We = n \cdot \mathrm{curl}\tau/\rho f_o$ is the Ekman pumping velocity. In Eq.(6), direct comparison between the effects of buoyancy flux and wind stress curl, represented by Wc and We in the expression of F, is possible. When the sum of these effects, F, is positive, positive vorticity is induced. For buoyancy flux, cooling is favorable for positive vorticity and for wind stress, positive curl is favorable for it because both effects cause the vortex stretching. The magnitude of both effects will be further discussed later.

Boundary condition for ψ is

$$\psi = \psi_B \tag{7}$$

where ψ_B is the value of ψ attributed along the lateral boundary as follows. Along the boundary connecting the left (right) edge of the inlet, $\psi = 0$ ($\psi = 1.0$) is attributed (c.f., Fig. 1). Along the eastern boundary section between the Soya and the Tsugaru Straits, ψ is specified as 1/3. This means that one third(two thirds) of the transport through the inlet passes through the Soya(Tsugaru) Strait(Fig. 1). Across the inlet and outlets, ψ varies linearly, meaning that no vorticity is assumed in these areas.

DECOMPOSITION INTO IM AND LM

The vorticity equation (6) with boundary condition (7) can be decomposed into Inflow-outflow Mode(IM), ψ_I, and Local Mode(LM), ψ_L, as follows:

$$\psi = \psi_I + \psi_L \tag{8}$$

where ψ_I and ψ_L denote IM and LM, respectively. The IM is governed by the homogeneous equation

$$\frac{\partial \psi_I}{\partial x} + C\nabla^2\psi_I = 0 \tag{9}$$

and satisfies the inhomogeneous boundary condition

$$\psi_I = \psi_B \text{ along the boundary} \quad (10)$$

The LM is governed by the inhomogeneous equation

$$\frac{\partial \psi_L}{\partial x} + C\nabla^2\psi_L = F \quad (11)$$

and satisfies the homogeneous boundary condition

$$\psi_L = 0 \text{ along the boundary} \quad (12)$$

The decomposition above has physical meanings as follows. The IM represents purely inflow-outflow driven circulation whereas the LM, the circulation driven purely by local forcing.

LOCAL FORCING

Let us first estimate the magnitude of the conversion rate Wc. It is expressed by

$$Wc = \frac{\alpha Q}{\rho C_p \Delta\rho} \quad (13)$$

where α/ρ is the thermal expansion coefficient, C_p is the heat capacity of sea water at constant pressure and Q is the amount of surface heat flux from sea to air. According to Manabe(1957), Q is more than 1000 ly/day(484 W/m^2 in MKS unit) in winter when cold air outbirsts from the Asian continent. Introducing the physical constants given in Table 1 into Eq.(13), this is equivalent to $W_C = 6 \times 10^{-6}$ m/s. If this cooling occurs for three months, the annual mean becomes $W_C \simeq 1.5 \times 10^{-6}$ m/s. In terms of F in Eq.(6), this is equivalent to $F \simeq 3.8$, using again the values given in Table 1.

According to Na et al.(1992),the annual mean wind stress curl is positive maximum of order 10^{-8} dyne/cm^3 in the northern/northwestern part of the basin and becomes smaller and negative toward the southeast. The maximum positive value corresponds to We of order 10^{-6} m/s and therefore to $F \simeq 2.5$ when the values in Table 1 are used.

Though the above estimations cannot be considered to be accurate, it can be accepted, without loss of generality, that the effects of both surface heat flux and wind are the same and have the same order of magnitude. In subsequent discussions,therefore, the type of local forcing will not be specified and various values of F, having the same order of magnitude as the above estimates, will be considered.

Table 1. Typical values used in estimation of F.

symbol	parameter	value	
f_o	Coriolis' parameter	10^{-4}	s^{-1}
β	beta constant	2×10^{-11}	$s^{-1}m^{-1}$
L	length scale	8×10^5	m
H	upper layer depth	10^2	m
*U	velocity scale	2.5×10^{-2}	m s^{-1}
α/ρ	thermal expansion	10^{-4}	K^{-1}
	coef.	10^{-4}	K^{-1}
$\Delta\rho$	vertical density	2	kg m^{-3}
	difference	2	kg m^{-3}
C_p	heat capacity at constant pressure	4×10^3	J $kg^{-1}K^{-1}$

*assumption is made that transport through inlet (UHL) is 2 Sverdrup.

Since the two local forcings are the strongest in the north, the functional form of F is taken to be exponential such that

$$F = F_o \ EXP[(y - y_N)/S] \quad (14)$$

where Fo is the magnitude of F; $y_N (=1.5)$, the y-position of the northern boundary; and S, the scale of forcing. Since the scales S is not known, various values will be considered. For comparison, step function F is also employed, which is given by

$$F = F_o \ (y_N - S) \le y \le y_N$$
$$F = 0 \ y < (y_N - S) \quad (15)$$

NUMERICAL SOLUTION

The vorticity equations (6), (9) or (11) with corresponding boundary conditions are solved using the successive overrelaxation method. The value of C in these equations is fixed at 0.1 throughout the calculations because it gives reasonable results (c.f., SK, 1989). The IM is found by solving the Eq.(9) with boundary condition (10).

The result(Fig. 3) shows a simple western and northern intensified current from the inlet to the

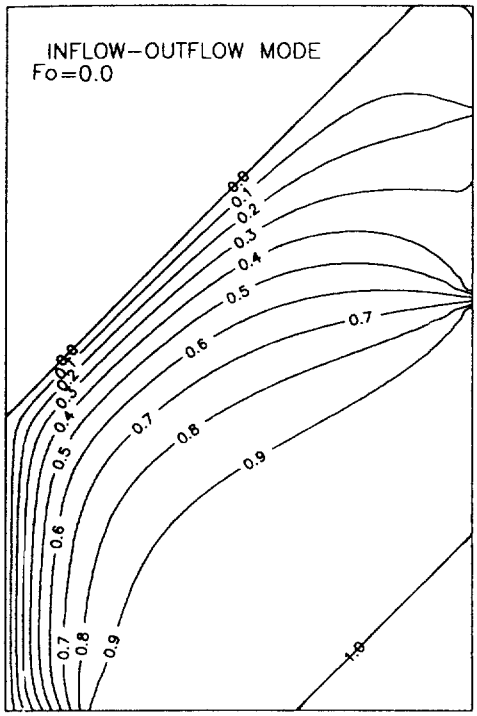

Fig. 3. Stream function of the inflow-outflow mode. Fo is the magnitude of the local forcing. All values are non-dimensionalized.

outlets. Similar results were obtained by Kang (1988) and SK(1989). The LM is computed from Eq.(11) with boundary condition (12). The combined circulation is found either by adding the two modes or by solving directly Eq.(6) with boundary condition (7). An example of solution for F=2.0 and S=1.0 is shown in Fig. 4. The LM is a cyclonic gyre residing in, and weakly around, the forcing region with western intensification. The combined circulation (IM+LM) shows a separation of inflow current on the western boundary where the two modes counterbalance. In the north of the separation position, southward current predominates along the westarn boundary, which then joins the recirculation cyclonic gyre forming in the north of the basin. As a contrasting example, the result for negative F with the same magnitude is also shown (Fig. 5). In this case, the LM has the same feature but the sense of rotation is opposite to that of positive F. The combined circulation is therefore a mere strengthening of the IM (Fig.

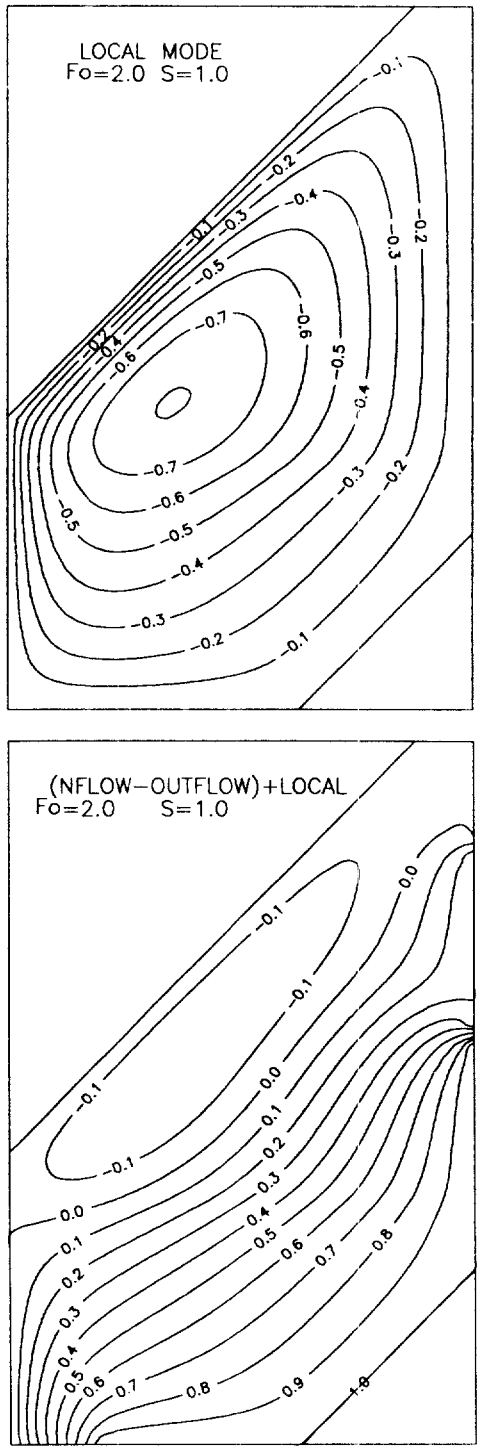

Fig. 4. Stream function of the local mode (upper) and the combined circulation (lower). S is the scale of the local forcing. All values are non-dimensionalized.

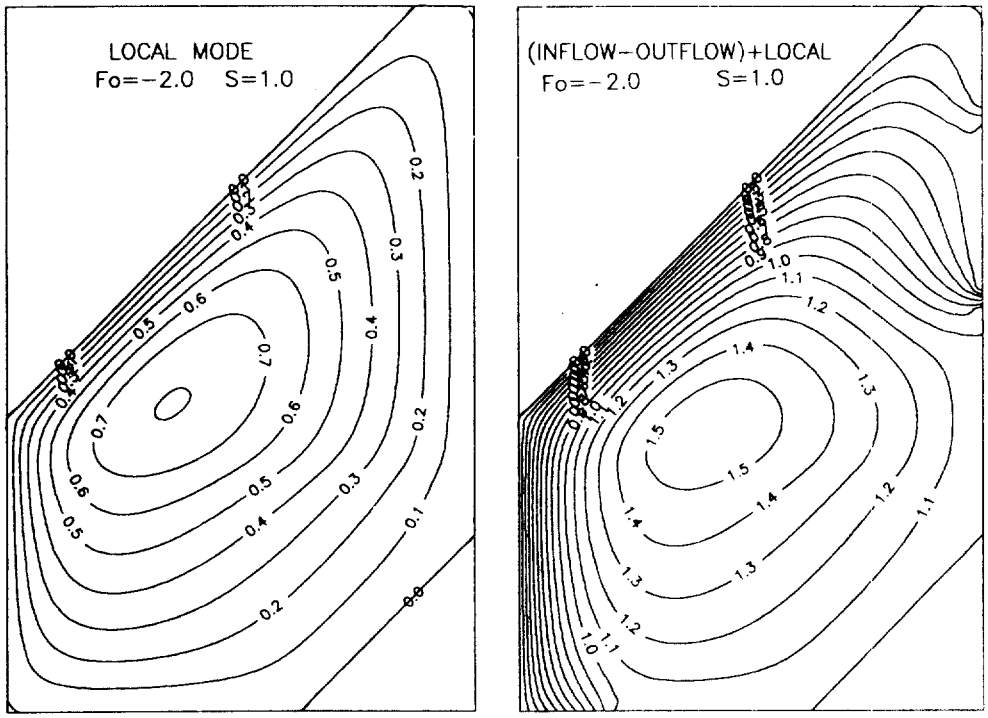

Fig. 5. Same as Fig.4 except for $F_o = -2.0$.

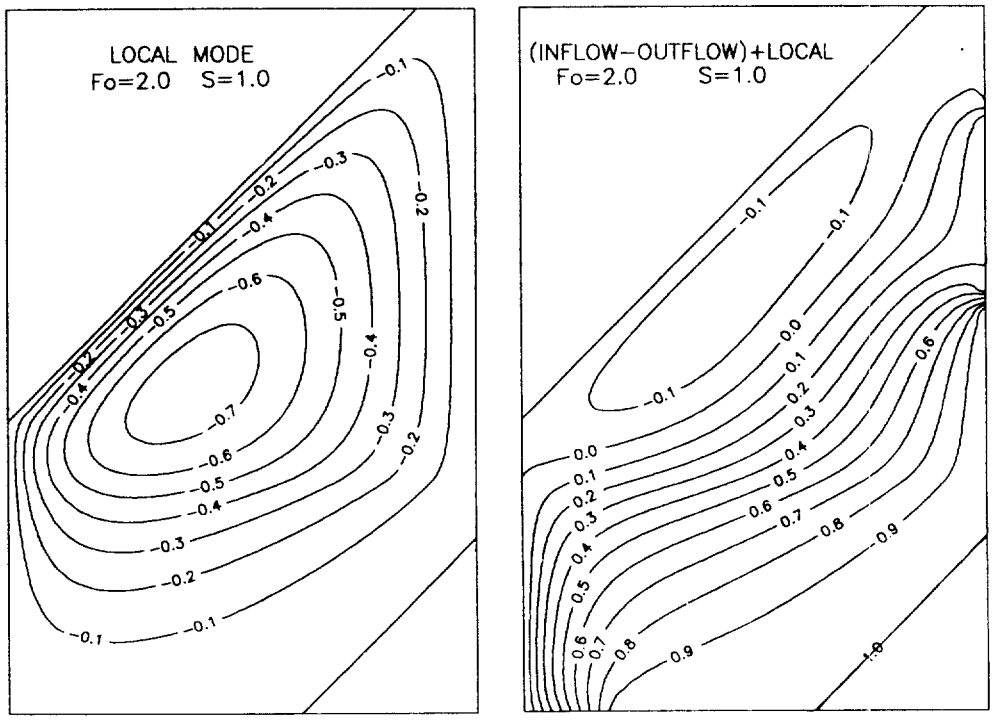

Fig. 6. same as Fig.4 except for using the step function forcing instead of exponential function forcing.

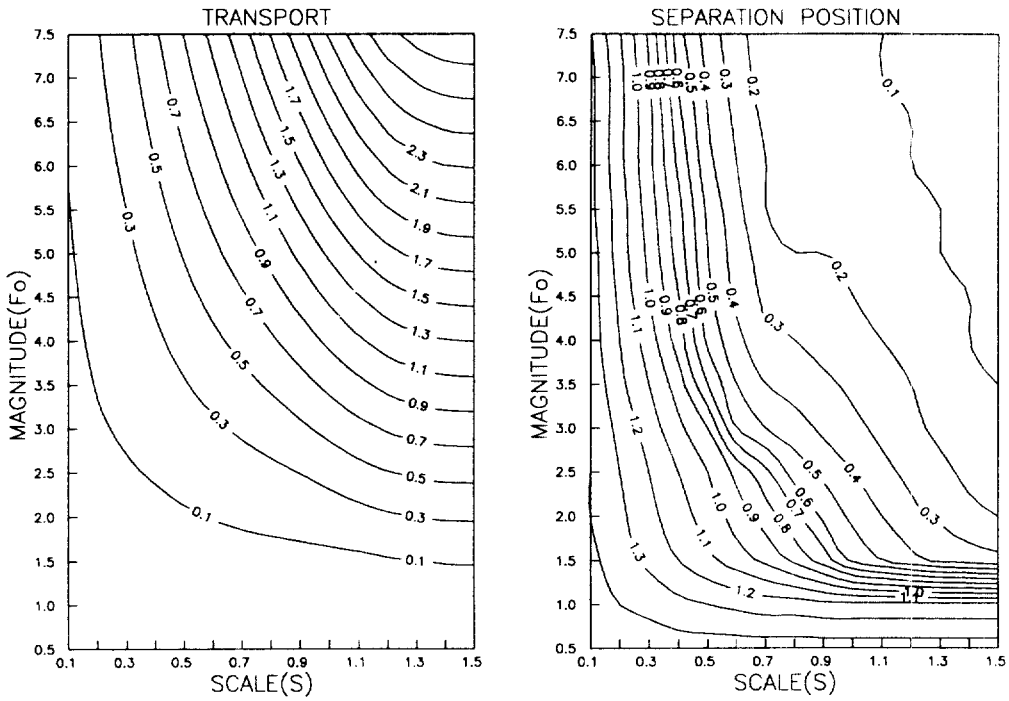

Fig. 7. Transport of cyclonic (recirculation) gyre and separation position (in y value) as functions of the magnitude and scale of the local forcing. All values are non-dimensionalized.

3) with a basin-wide anti-cyclonic gyre in the interior. Experiments with step function F give nearly the same results as those of exponential function F. The difference is that for the step F, extension of circulation outside the forcing region is slightly weaker(compare Fig. 4 and Fig. 6).

The dependence of the separation position and the strength of the recirculation gyre on the magnitude, Fo, and the scale, S is shown in Fig.7. The strength of the recirculation gyre, represented by total transport, increases and the separation position moves southward with increase of the magnitude and scale; for small magnitude (scale), however, the separation position becomes insensitive to the scale(magnitude). In fact, it is quite normal to expect that the oceanic response amplifies and extends in accordance with the magnitude and scale of the forcing, respectively. In the East Sea, the reasonable separation position of EKWC may correspond to about y=0.5 although the transport of recirculation gyre(associated with NKCC) is quite uncertain. The case of F=2.0 and S=1.0 considered previously seems therefore relevant to the East Sea.

CONCLUDING REMARKS

Within the context of the simple model considered here, the separation of EKWC and the generation of NKCC are due to the local forcing which is favorable for the vortex stretching. This can be achieved either by surface cooling or by positive wind stress curl. The northern part of the East Sea is known as the area of deep/intermediate water formation and surface cooling is expected to be large. In fact, the heat balance of the East Sea seems mostly between surface cooling and horizontal advection of heat by inflowing warm current. The wind stress curl is known to be mostly positive, especially in the north where the major part of local mode is formed (Na et al.,1992). It can be deduced therefore that the separation of EKWC and the formation of NKCC is caused both by the surface cooling and the wind.

Present knowledges about the surface boundary conditions of the East Sea are, however, still quite insufficient to be used in drawing definite conclusions. Especially, more accurate estimation of surface cooling is prerequisite to better understanding of the circulation of the East Sea. On the other hand, some essential features may be missed by the idealization of the problem made here, such as the two-layer assumption, neglect of non-linearity and parameterization of friction etc. This study is therefore considered to be just one step toward the better understanding of the dynamics of the East Sea circulation. More complete modelling of the circulation of the East Sea can be considered as the next step.

ACKNOWLEDGEMENTS

This study is an output of 1990-1993 research program supported by KOSEF. The author acknowledges the comments made by referees.

REFERENCES

Hong, C.H., K.D. Cho and S.K. Yang, 1984. On the abnormal cooling phenomenon in the coastal areas of East Sea of Korea in Summer 1981. *J. Oceanol. Soc. Korea*, **19**: 11-17.

Hydrographic Office of Korea, 1982. Marine environmental atlas of Korean Waters. Pub. No. 1451.

Kang, Y.Q., 1988. On the formation of the East Korean Warm Current. *Ocean Research*, **10**: 1-6.

Kim, k. and R. Legeckis, 1986. Branching of the Tsushima Current in 1981-83. *Prog. Oceanoogr.*, **17**: 265-276.

Lim, C.H. and H.S. An, 1985. The comparison of the volume transport in the Korea Strait and in the Middle of the East Sea(Japan Sea). *J. Oceanol. Soc. Korea*, **20**: 50-55.

Manabe, S., 1957. On the modification of air-mass over the Japan Sea when the outburst of cold air predominates. *J. Met. Soc. Japan, Ser.*, **35**: 311-326.

Na, J.Y., J.W. Seo and S.K. Han, 1992. Monthly-mean sea surface winds over the adjacent seas of the Korean peninsular. *J. Oceanol. Soc. Korea*, **27**: 1-10.

Sekine, Y., 1986. Wind-driven circulation in the Japan Sea and its influence on the branching of the Tsushima Current. *Prog. Oceanogr.*, **17**: 297-312.

Seung, Y.H. and K. Kim, 1989. On the possible role of local thermal forcing on the Japan Sea circulation. *J. Oceanol. Soc. Korea*, **24**: 29-38.

Uda, M., 1934. The results of simultaneous oceanographical investigations in the Japan Sea and its adjacnt waters in May and June, 1932. *J. Imp. Fish. Exp. Sta.*, **5**: 57-190 (in Japanese).

U.S. Navy, 1977. Marine climate atlas of the world, Vol.: North Pacific Ocean. Naval Weather Service Detachment, Asheville. N.C., NAVAIR 50-1C-529.

Yoon, J.H., 1982a. Numerical experiment on the circulation in the Japan Sea, Part: Formation of the East Korean Warm Current. *J. Oceanogr. Soc. Japan*, **38**: 43-51.

Yoon, J.H., 1982b. Numerical experiment on the circulation in the Japan Sea, Part: Formation of the near shore branch of the Tsushima Current. *J. Oceanogr. Soc. Japan*, **38**: 119-124.

Accepted June 17, 1992